Published in final edited form as:

J Med Genet. 2020 September ; 57(9): 634–642. doi:10.1136/jmedgenet-2019-106615.

MicroRNA-4516-mediated regulation of *MAPK10* relies on 3'UTR *cis*-acting variants and contributes to the altered risk of Hirschsprung disease

Yang Wang[#1,3,4,*], **Qian Jiang**[#2], **Aravinda Chakravarti**[5], **Hao Cai**[1,3,4], **Ze Xu**[1,3,4], **Wenjie Wu**[1,3,4], **Beilin Gu**[1,3,4], **Long Li**[6,*], **Wei Cai**[1,3,4,*]

[1]Department of Pediatric Surgery, Xinhua Hospital, School of Medicine, Shanghai Jiao Tong University, Shanghai, China

[2]Department of Medical Genetics, Capital Institute of Pediatrics, Beijing, China

[3]Shanghai Key Laboratory of Pediatric Gastroenterology and Nutrition, Shanghai, China

[4]Shanghai Institute for Pediatric Research, Shanghai, China

[5]Center for Human Genetics and Genomics, New York University School of Medicine, New York, NY, USA

[6]Department of General Surgery, Capital Institute of Pediatrics Affiliated Children's Hospital, Beijing, China

[#] These authors contributed equally to this work.

Abstract

Background—Hirschsprung disease (HSCR) is a life-threatening congenital disorder in which the enteric nervous system (ENS) is completely missing from the distal gut. Recent studies have shown that miR-4516 markedly inhibits cell migration, and as one of its potential targets, *MAPK10* functions as a modifier for developing HSCR. We thus aimed to evaluate the role of miR-4516 and *MAPK10* in HSCR and how they contribute to the pathogenesis of HSCR.

Methods—We examined 13 genetic variants using the MassArray system in a case-control study (n = 1015). We further investigated miR-4516-mediated regulation of MAPK10 in HSCR cases and human neural cells, the effects of *cis*-acting elements in MAPK10 on miR-4516-mediated modulation and cell migration process.

[*]Correspondence should be addressed to: Dr Wei Cai, Department of Pediatric Surgery, Xin Hua Hospital, 1665 Kongjiang Road, Shanghai 200092, P.R. China, Tel & Fax: +86 (0) 21 25076449 caiw204@sjtu.edu.cn or Dr Long Li, Department of General Surgery, Capital Institute of Pediatrics Affiliated Children's Hospital, 2 Yabao Road, Beijing 100020, P.R. China, lilong23@126.com or Dr Yang Wang, Department of Pediatric Surgery, Xin Hua Hospital, 1665 Kongjiang Road, Shanghai 200092, P.R. China, Tel & Fax: +86 (0) 21 25076449 wangyang@xinhuamed.com.cn.

Contributions

YW, QJ, LL and WC designed the study. YW, HC and ZX performed the experiments. QJ, WW and BG collected the samples. YW, QJ, LL and WC analyzed the data. YW, QJ and AC wrote the manuscript. LL and WC supervised the study. All authors approved the final manuscript.

Competing interests

None declared.

Results—Three positive 3'UTR variants in *MAPK10* were associated with altered HSCR susceptibility. We also showed that miR-4516 directly regulates *MAPK10* expression, and this regulatory mechanism is significantly affected by the 3'UTR *cis*-acting elements of *MAPK10*. Additionally, knock-down of *MAPK10* rescued the effect of miR-4516 on the migration of human neural cells.

Conclusion—Our findings indicate a key role of miR-4516 and its direct target *MAPK10* in HSCR risk, and highlight the general importance of *cis*- and posttranscriptional modulation for HSCR pathogenesis.

INTRODUCTION

The enteric nervous system (ENS), sometimes referred to as the "second brain", is derived from neural crest cells (NCCs) which originate from the dorsal neural tube and migrate over a long distance to the gut.[1] Disturbances in the ENS development may result in Hirschsprung disease (HSCR, MIM 142623), a life threatening genetic disorder, in which the ENS is completely missing from distal bowel (aganglionosis).[2] Based on the extent of aganglionosis, HSCR is classified as short segment HSCR (S-HSCR), long segment HSCR (L-HSCR) and total colonic aganglionosis (TCA), and S-HSCR accounts for about 80% of HSCR cases.[3] With an incidence of approximately 1/5000 newborns worldwide (2.8/10000 newborns in Asian population), HSCR is the most frequent congenital disorder of intestinal motility.[4]

Importantly, HSCR also shows classical features of multifactorial genetic models, including high heritability (> 80%), high sibling recurrence risk (200-fold greater than the normal population), dramatic sex bias (~ 4:1 affected males : females), and complex inheritance patterns in families.[5] Genetic studies so far have shown that more than 15 genes might be linked to HSCR etiology, including RET (receptor tyrosine kinase), GDNF (glial cell derived neurotrophic factor), and EDNRB (endothelin receptor type B), the major HSCR susceptibility genes.[67] However, these genes cumulatively accounts for < 10% of cases.[8] and only about 0.1% of the heritability in HSCR can be attributed to the genetic variants within these genes, indicating more genes with incomplete penetrance might be implicated in HSCR pathology.[9] A recent study has identified a genetic interaction between *mapk10* (mitogen-activated protein kinase 10) and *ret* in a zebrafish model, and actually introduction of *mapk10* mutations into *ret* heterozygous zebrafish enhanced the ENS deficit, suggesting *MAPK10* as a HSCR susceptibility locus.[10] Additionally, it has been unraveled that an intronic 3.5 kb deletion within *MAPK10* might be a potential modifier for developing HSCR.[11]

microRNAs (miRNAs) are small non-coding RNA molecules that post-transcriptionally modulate gene expression by promoting mRNA degradation and/or repressing translation, and thus play key roles in various physiological and pathological conditions, including neuronal differentiation, plasticity, development, survival, and central nervous system disorders.[1213] More recent studies have focused on the miRNAs-mediated regulation of cell migration in the enteric nervous system, and dozens of miRNAs are demonstrated to be linked to HSCR etiology.[1415] Interestingly, recent work reveals that miR-4516 may be

involved in the mechanism of suppression of cell migration, and actually loss of miR-4516 expression contributes to accelerated migration in keratinocytes.[16,17]

Based on the 1015 subjects, we here demonstrate that *MAPK10*, as a direct target of miR-4516, is linked to the altered HSCR susceptibility, and over-expression of miR-4516 markedly hinders the migration of human neural cells. Surprisingly, we also observes that *cis*-acting haplotype can further affect miR-4516-mediated regulation of *MAPK10*. These results indicate that miR-4516 modulates neural cell migration via a *MAPK10*-dependent way, and implicate a *cis*-acting dependent regulatory mechanism mediated by miR-4516 in HSCR etiology.

METHODS

Participants

1015 subjects were recruited in the present study, including 502 cases with HSCR (383 males and 119 females) and 513 normal controls (310 males and 203 females). The mean ages of case group and control group were 1.34 ± 2.12 years and 2.70 ± 3.13 years, respectively. All the participants enrolled in the study were biologically unrelated residents who were of Han Chinese origin. The characteristics of the study population are summarized in table S1. The 502 HSCR cases were diagnosed according to histological examination of biopsy/surgical resection material for the absence of ganglion cells, and consisted of 369 subjects of S-HSCR (short segment SHCR), 74 subjects of L-HSCR (long segment HSCR) and 59 subjects of TCA (total colonic aganglionosis). For HSCR tissues, we utilized the normoganglionic dilated segment of the HSCR colon in the present study. We randomly recruited controls from the subjects with no history of chronic constipation. The study was reviewed and approved by the ethics committee of both Xinhua Hospital and Capital Institute of Pediatrics (Reference XHEC-D-2011–022 and SHERLL 2013039). Written informed consent was provided by participants or their parents after the procedure had been fully explained. All experiments were performed in accordance with the tenets of the Declaration of Helsinki. DNA samples were extracted by using the QIAamp DNA blood midi kit (Qiagen, Valencia, CA).

SNP selection and genotyping

We performed the tagSNP selection using the Genome Variation Server (http://gvs.gs.washington.edu/GVS150/) with MAF (minor allele frequency) ≥ 0.2 and $r^2 \geq 0.8$ based on the HapMap HCB (Han Chinese in Beijing) data. In the study, we recruited 13 tagSNPs within *MAPK10*, including 3’ UTR SNPs (rs958, rs2589515, rs1201, rs7699978 and rs2575675) and 8 intronic SNPs (rs2869444, rs6823664, rs12644920, rs4693765, rs17449147, rs10021706, rs1898248 and rs1946733) (figure S1). The MassARRAY iPLEX Gold technology (Sequenom, San Diego, CA) was used for conducting genotyping, and multiple criteria are included for genotyping quality control, similar to previous methods.[18] Representative mass spectra of the 13 genetic variants within *MAPK10* were shown in figure S2.

Cell cultures and transfections

The human neuroblastoma SH-SY5Y cells, which have been used as HSCR cell model,[15] were maintained in Dulbecco's Modified Eagle Medium (DMEM)/Nutrient Mixture F-12 supplemented with 10% fetal bovine serum (FBS), and passaged by trypsinization. The miR-4516 inhibitor, scramble control, miR-4516 mimics, control mimics, siRNA for *MAPK10* and control siRNA were purchased from GenePharma (Shanghai, China). We utilized qRT-PCR to assess the MAPK10 silencing effectiveness of all the three candidate siRNAs, and found that si-MAPK10–3 was the most effective one (figure S3), which thus was used in the present study. Transfections of miRNA inhibitors and mimics and siRNAs (at 50 nM final concentration) were conducted with lipofectamine 2000 (Thermo Fisher Scientific). SH-SY5Y cells were transfected for 6 hours, and the efficiency of transfections was 90% - 95%.

Quantitative real-time PCR (qRT-PCR) and Western blotting analysis

Total RNA was extracted from tissues and cell cultures with TRIZOL (Invitrogen, MA, USA), according to the manufacturer's instructions. For miRNA, Universal cDNA Synthesis Kit II, ExiLENT SYBR® Green master mix and custom-designed LNA primers (Exiqon) were included, and the miRNA levels were normalized to the uniformly expressed U6 snRNA. For mRNA, we used RevertAid First Strand cDNA Synthesis Kit and PowerUp SYBR Green Master Mix (Thermo Fisher Scientific). The mRNA levels were monitored by qRT-PCR with specific primers (Supplementary table S2) on the QuantStudio system (Thermo Fisher Scientific). Threshold cycles (Cts) were generated automatically, and the relative expressions were shown as $2^{-\Delta Ct}$. Relative mRNA levels were normalized to the reference gene *ACTB*. Proteins have been harvested and Western blotting analysis has been conducted as described previously.[19] The following primary antibodies were used according to the manufacturer's instructions: mitogen-activated protein kinase 10 (MAPK10) (Santa Cruz, TX, USA, 1:1000), and glyceraldehyde-3-phosphate dehydrogenase (GAPDH) (Santa Cruz, TX, USA, 1:5000).

MiR-4516 target validation and cis-regulation analysis by luciferase reporter assay

To validate the predicted miR-4516 binding site, a fragment of MAPK10 3' UTR or a double mutated sequence of the predicted target sites were inserted into the XbaI site of pGL3 promoter vector, and for *cis*-regulation analysis, the *MAPK10* 3' UTR containing either the haplotype ACT (rs1201-rs7699978-rs2575675) or GAC (rs1201-rs7699978-rs2575675) was inserted into the XbaI site of pGL3 promoter vector (Genechem, Shanghai, China). By using lipofectamine 2000 (Thermo Fisher Scientific), the constructs were co-transfected with either miR-4516 mimics, or control mimics (50 nM final concentration) to the SH-SY5Y cells. 48 h after transfections, luciferase luminescence (firefly and renilla) was measured by the Dual-Luciferase® Reporter Assay System (Promega).

Wound healing assay

Confluent transfected SH-SY5Y cells were linear scratch wounded with a P200 pipette tip following a previous described method.[20] Incubation was continued for an additional 24 h. Images were taken at 0 h and 24 h and analyzed by using the ImageJ software. Cell

migration was quantified using the following equation: (0 h wound area - 24 h wound area) / 0 h wound area ×100. Cell migration values under each condition was normalized to the appropriate control, and average percent migration was obtained in three independent assays.

Statistical analysis

We conducted the unpaired, 2-tailed Student t-test for comparison among two groups by using GraphPad Prism 6 (GraphPad Software, CA, USA). Hardy-Weinberg equilibrium, allelic and genotypic association, and haplotype distribution were assessed as described previously.[18] Images in the present study were quantified with ImageJ Software (version 1.49j, NIH). The difference between comparisons was considered to be statistically significant when $P < 0.05$. All values were shown as mean ± SEM.

RESULTS

Association of genetic variants with HSCR

Genotype distributions of all 13 polymorphisms presented no significant deviations from Hardy-Weinberg equilibrium in either HSCR or control group ($P > 0.05$). There were significant associations between HSCR and 8 genetic variants within *MAPK10*, and we observed that the significance in allele distributions of the 3 positive SNPs (rs10021706, rs1201 and rs2575675) remained after the FDR correction (table 1). Moreover, the A allele of rs10021706, the A allele of rs1201 and the T allele of rs2575675 showed significantly higher frequencies in HSCR group compared to control group. These findings in the 3 positive variations remained significant with adjustment for gender and age factors using the PLINK software ($P < 0.05$).

We then conducted haplotype analyses of polymorphisms in *MAPK10* gene since haplotypes constructed from genetic variants with strong linkage disequilibrium will increase the statistical power for association with the disease. Strong LD ($D' > 0.7$) was observed in the following groups, rs2869444-rs6823664-rs12644920-rs4693675-rs17449147, and rs1898248-rs1946733-rs958-rs2589515-rs1201-rs7699978-rs2575675 (figure S4). Accordingly, we further assessed haplotypes with strong LD and found that several haplotypes were strongly associated with HSCR (table 2). Haplotype analysis also revealed some significant global *P* values, and specifically, the haplotype, rs1201-rs7699978-rs2575675, was the most significant ($P = 0.0006$) (table S3).

MAPK10 mRNA correlates inversely with miR-4516 in HSCR

Since genetic variants within *MAPK10* were strongly associated with HSCR, we further examined the expression of *MAPK10* in 92 HSCR subjects and 92 controls. As shown in figure 1A, *MAPK10* mRNA expression was significantly reduced in HSCR tissues compared to controls. Additionally, we identified *MAPK10* as one of the putative targets for miR-4516 by employing several target prediction algorithms. MiR-4516 shows potential for the base-pairing with MAPK10 mRNA, based on the extended 5' 7-mer-seed and an additional 3' binding (figure 1F). To test whether reduced MAPK10 level can be attributed to miR-4516 over-expression in HSCR, we thus assessed the expression of miR-4516 in HSCR and control group, and found miR-4516 expression was significantly increased in

HSCR (figure 1B). In addition, the increased levels of miR-4516 expression in HSCR tissues correlated inversely with MAPK10 mRNA expression (figure 1C, $R^2 = 0.3162$, $P < 0.0001$).

Validation of MAPK10 as a direct target of miR-4516

To examine whether human MAPK10 is modulated by miR-4516, we further interrogated its expression in human SH-SY5Y neuroblastoma cells, which were transfected with either miR-4516 inhibitors or mimcs. As assessed by qRT-PCR and Western blotting, over-expression of miR-4516 markedly reduced the levels of MAPK10 mRNA and protein, whereas miR-4516 inhibition significantly increased these levels (figure 1D and 1E).

To validate that MAPK10 is a direct target of miR-4516, we cloned a fragment of human MAPK10 3' UTR containing the predicted miR-4516 binding site to a pGL3 promoter vector, and co-transfected this construct with either miR-4516 mimics or control mimics into SH-SY5Y cells. Compared to the control mimic, co-transfection of miR-4516 with wild type MAPK10 3' UTR markedly reduced the activity of the reporter gene, and this regulation was dramatically abolished by the mutation within the miR-4516 binding site (figure 1F and 1G), indicating that miR-4516 binds directly to MAPK10 3' UTR and downregulates MAPK10 expression.

Cis-acting haplotype altered miR-4516-mediated regulation of MAPK10

Since genetic variants located in the 3' UTR either enhance or disrupt miRNA binding and target regulation (i.e. the *cis*-acting variants),[21] we next attempted to assess the effects of polymorphisms or haplotypes within the 3'UTR of *MAPK10* on miR-4516-mediated modulation of gene expression. For the 92 HSCR subjects, the levels of *MAPK10* expression in the 63 cases carrying the A-C-T haplotype (rs1201-rs7699978-rs2575675) were significantly lower than those in the 2 cases carrying the G-A-C haplotype (rs1201-rs7699978-rs2575675). Moreover, we also found that the GG genotype (rs1201) individuals showed markedly higher *MAPK10* expression than AA or GA genotype individuals. For rs7699978, the AA genotype subjects presented strongly increased expression of *MAPK10* compared to CA or CC genotype subjects. Regarding rs2575675, the CC genotype carriers showed significantly higher *MAPK10* expression than the TT genotype carries, whereas there were no markedly differences in *MAPK10* expression between CC and TC genotype carriers (figure 2A–D).

Additionally, a fragment of human MAPK10 3' UTR bearing the haplotype (rs1201-rs7699978-rs2575675, A-C-T or G-A-C) was cloned to a pGL3 promoter vector, and co-transfected with either miR-4516 mimics or control mimics into SH-SY5Y cells. Compared to the G-A-C haplotype, the A-C-T haplotype facilitated the repression of miR-4516 on luciferase reporter, whereas these effects on the reporter were not observed after the human neural cells were transfected with the control mimics (figure 2E).

MiR-4516 regulates the migration of human neural cells through MAPK10-dependent way

To test the effects of miR-4516 on migration of human neural cells, we assessed the cell migration process by over-expressing or inhibiting miR-4516 in SH-SY5Y cells. Of note, 24h after confluent transfected SH-SY5Y cells were linear scratch wounded, over-

expression of miR-4516 in SH-SY5Y cells led to a significant reduction in cell migration ($P = 0.0031$), whereas its inhibition strongly stimulated cell migration ($P = 0.0063$) (figure 3A). We then further interrogated whether the effects of miR-4516 on cell migration were mediated by MAPK10. Therefore, we co-transfected SH-SY5Y cells with miR-4516 inhibitor and the siRNA cognate to MAPK10 mRNA. Interestingly, wound healing assays demonstrated that MAPK10-targeting siRNA rescued the effects of miR-4516 on cell migration (figure 3B), indicating that miR-4516 modulates cell migration and this modulation is mediated by MAPK10 in human neural cells.

DISCUSSION

In the current study, we initiated a LD analysis of 13 genetic variants within *MAPK10* in 1015 subjects (502 HSCR cases and 513 normal controls), and our findings indicated a strong association of *MAPK10* with the altered risk of Hirschsprung disease. Since 5 out of the 8 polymorphisms linked to HSCR are located in the untranslated region (figure S1), they may play a key role in the regulatory mechanisms of gene expression.[22] Additionally, the A allele of rs10021706, the A allele of rs1201 and the T allele of rs2575675 were more common in HSCR cases compared to normal controls, suggesting that all might be the risk factors for HSCR. It has also been reported that *MAPK10* might be involved in the development of the enteric nervous system, and this gene might be a potential HSCR susceptibility locus,[10] which was further supported by our present data.

On the other hand, aberrant expression of specific microRNAs has been linked to a wide range of human diseases. Although these miRNAs often explain profound pathological effects in terms of disease initiation and progression, their functions in Hirschsprung disease have not been fully delineated yet. We here identified *MAPK10* as a potential target of miR-4516, and our results indicate that up-regulation of miR-4516, observed in HSCR, contributes to the decreased MAPK10 expression (figure 1).

MiR-4516, located in the cytoplasm[23], has important regulatory functions in multiple pathological conditions, such as HIV-associated neurocognitive disorder (HAND), thyroid carcinomas, and lung cancer.[24–26] Meanwhile, some targets and signaling pathways may underlie miR-4516-mediated functions. Interestingly, over-expression of miR-4516 in human keratinocytes inhibits cell motility and proliferation through down-regulation of genes involved in cytoskeletal reorganization, and in response to PUVA (8-Methoxypsoralen plus UVA), miR-4516 also mediates inactivation of AKT/mTOR pathway followed by suppression of cell migration.[1617] Moreover, miR-4516 modulates intercellular junctions by targeting PVRL1 (poliovirus receptor related protein 1).[27]

In the present study, we provide solid evidence that MAPK10 is a novel target of miR-4516, and the elevated level of miR-4516 results in down-regulation of MAPK10 in human neural cells (figure 1A–E), for the first time. A recent study has shown that *Mapk10* is highly expressed in ENS cells during mouse development. [28] Accordingly, we recruited the normoganglionic dilated segment of the HSCR colon to assess the expression levels of MAPK10 and miR-4516, and this reduced MAPK10 expression identified in HSCR cases might indicate the altered regulation of MAPK10 in the progression of Hirschsprung

disease. Importantly, we have found that miR-4516 directly modulates MAPK10. As shown in Luciferase assay, up-regulation of miR-4516 led to significant inhibition of MAPK10, whereas the mutated miR-4516 binding site caused de-repression of this target in SH-SY5Y cells (figure 1G). It is more likely that a deletion identified in *MAPK10* gene acts as a modifier of Hirschsprung disease.[11] MAPK10 regulates neuronal differentiation via phosphorlation of APP (amyloid precursor protein) and STMN2 (stathmin2), and loss of MAPK10 may affect APP and/or STMN2 signaling during the process of enteric neuron differentiation, and may thus contribute to HSCR risk.[2930]

Since haplotype analysis may increase the power to detect disease loci compared to individual SNP analysis under certain conditions,[31] the positive haplotype we observed here might also account for the altered risk of HSCR (table 2). Interestingly, the most significant window spanned 3 genetic variants (rs1201-rs7699978-rs2575675) in *MAPK10*, and the A-C-T haplotype (rs1201-rs7699978-rs2575675) might be a potential risk factor for HSCR ($P = 2.94 \times 10^{-4}$, OR = 1.46, 95% CI 1.19–1.79). On the other hand, genetic variations in the 3'UTR region may change the complementarity between a miRNA and its target gene (s), and therefore may affect the accessibility of miRNA binding sites. At this point, these 3' UTR SNPs or haplotypes, as cis-regulatory elements, may further influence the expression levels of the target gene (s).[32] All these clues led us to further assess how haplotypes or individual SNPs located in the 3' UTR region affected miR-4516-mediated regulation of *MAPK10* expression. Regarding rs1201-rs7699978-rs2575675, the A-C-T haplotype or individual genotypes (i.e. AA for rs1201, CC for rs7699978, and TT for rs2575675) facilitated the binding of miR-4516 to *MAPK10* compared to the G-A-C haplotype or other corresponding genotypes, causing a decreased level of *MAPK10* expression. In human neural cells, we also confirmed that the A-C-T haplotype promoted the miR-4516 modulation of the MAPK10 3' UTR. These lines of evidence indicate that cis-acting elements within *MAPK10* might further contribute to HSCR pathogenesis. With respect to the *MAPK10* expression analyses in various haplotypes or genotypes, our sample size is relatively small. Due to the preponderance of the major haplotype/genotype carriers compared to the minor haplotype/genotype carriers in HSCR, it is difficult to get a balanced representation of all haplotypes/genotypes and a desirable sample size. Therefore, additional replication studies with larger samples will certainly be needed in the future.

The ENCC migration is crucial to the development of ENS. Since the gut is growing in length as the cells migrate, the ENCCs probably migrate further than any other kind of embryonic cell population.[33] However, the ENCCs do not always complete their journey along the entire intestine, and it may lead to HSCR phenotypes once their migration is hindered. In the present study, we have shown that up-regulation of miR-4516 markedly slows down the migration of human neural cells, and a similar effect has recently been demonstrated in keratinocytes.[16] *MAPK10*, as a direct target of miR-4516, has also been proved to modulate the development of enteric nervous system in a zebrafish model.[10] Interestingly, the effects of miR-4516 on neural cell migration were rescued when we knocked down the level of MAPK10 expression by using the specific siRNA. Though MAPK10 is a key player in the modulation of cell migration by miR-4516, whether the expression levels of MAPK10 and miR-4516 are changed not only in neural cells but in

other types of cells in HSCR, and if so how their altered levels in these cells affect the disease progression, remains to be further investigated.

Collectively, these data indicate that up-regulation of miR-4516 along with reduced *MAPK10* expression may unravel the potential risk factors for HSCR. Since a genetic interaction between *mapk10* and *ret* supports for a model in which *mapk10* mutations modify RET activity and HSCR disease presentation,[10] our present study shows additional complexity that stems from cis-acting elements and posttranscriptional modulation. Although understanding the full extent of miR-4516 regulation in the pathogenesis of HSCR needs further investigation, our findings suggest a key role played by miR-4516 and MAPK10 in HSCR risk, and underline the general importance of *cis*- and posttranscriptional modulation for HSCR pathogenesis.

Supplementary Material

Refer to Web version on PubMed Central for supplementary material.

Acknowledgements

We thank all the members for their contributions to the present study.

Funding

This work was supported by the National Nature Science Foundation of China (81670469, 81630039 and 81771620), SMC-Chenxing Young Scholar Program of Shanghai Jiao Tong University, Shanghai Key Laboratory of Pediatric Gastroenterology and Nutrituion (17DZ2272000), Beijing Hospital Administration “Peak Climbing” Talents Development Program (DFL20181301) and Shanghai Municipal Health Commission (201840028).

REFERENCES

1. Young HM, McKeown SJ. Motility: Hirschsprung disease--laying down a suitable path. Nat Rev Gastroenterol Hepatol 2016;13:7–8. [PubMed: 26701374]
2. Avetisyan M, Schill EM, Heuckeroth RO. Building a second brain in the bowel. J Clin Invest 2015;125:899–907. [PubMed: 25664848]
3. Amiel J, Sproat-Emison E, Garcia-Barcelo M, Lantieri F, Burzynski G, Borrego S, Pelet A, Arnold S, Miao X, Griseri P, Brooks AS, Antinolo G, de Pontual L, Clement-Ziza M, Munnich A, Kashuk C, West K, Wong KK, Lyonnet S, Chakravarti A, Tam PK, Ceccherini I, Hofstra RM, Fernandez R, Hirschsprung Disease C. Hirschsprung disease, associated syndromes and genetics: a review. J Med Genet 2008;45:1–14. [PubMed: 17965226]
4. Gfroerer S, Rolle U. Pediatric intestinal motility disorders. World J Gastroenterol 2015;21:9683–7. [PubMed: 26361414]
5. Badner JA, Sieber WK, Garver KL, Chakravarti A. A genetic study of Hirschsprung disease. Am J Hum Genet 1990;46:568–80. [PubMed: 2309705]
6. Wallace AS, Anderson RB. Genetic interactions and modifier genes in Hirschsprung’s disease. World J Gastroenterol 2011;17:4937–44. [PubMed: 22174542]
7. Tilghman JM, Ling AY, Turner TN, Sosa MX, Krumm N, Chatterjee S, Kapoor A, Coe BP, Nguyen KH, Gupta N, Gabriel S, Eichler EE, Berrios C, Chakravarti A. Molecular Genetic Anatomy and Risk Profile of Hirschsprung’s Disease. N Engl J Med 2019;380:1421–32. [PubMed: 30970187]
8. Jiang Q, Arnold S, Heanue T, Kilambi KP, Doan B, Kapoor A, Ling AY, Sosa MX, Guy M, Jiang Q, Burzynski G, West K, Bessling S, Griseri P, Amiel J, Fernandez RM, Verheij JB, Hofstra RM, Borrego S, Lyonnet S, Ceccherini I, Gray JJ, Pachnis V, McCallion AS, Chakravarti A. Functional loss of semaphorin 3C and/or semaphorin 3D and their epistatic interaction with ret are critical to Hirschsprung disease liability. Am J Hum Genet 2015;96:581–96. [PubMed: 25839327]

9. Emison ES, Garcia-Barcelo M, Grice EA, Lantieri F, Amiel J, Burzynski G, Fernandez RM, Hao L, Kashuk C, West K, Miao X, Tam PK, Griseri P, Ceccherini I, Pelet A, Jannot AS, de Pontual L, Henrion-Caude A, Lyonnet S, Verheij JB, Hofstra RM, Antinolo G, Borrego S, McCallion AS, Chakravarti A. Differential contributions of rare and common, coding and noncoding Ret mutations to multifactorial Hirschsprung disease liability. Am J Hum Genet 2010;87:60–74. [PubMed: 20598273]
10. Heanue TA, Boesmans W, Bell DM, Kawakami K, Vanden Berghe P, Pachnis V. A Novel Zebrafish ret Heterozygous Model of Hirschsprung Disease Identifies a Functional Role for mapk10 as a Modifier of Enteric Nervous System Phenotype Severity. PLoS Genet 2016;12:e1006439. [PubMed: 27902697]
11. Jiang Q, Ho YY, Hao L, Nichols Berrios C, Chakravarti A. Copy number variants in candidate genes are genetic modifiers of Hirschsprung disease. PloS One 2011;6:e21219. [PubMed: 21712996]
12. Olde Loohuis NF, Kos A, Martens GJ, Van Bokhoven H, Nadif Kasri N, Aschrafi A. MicroRNA networks direct neuronal development and plasticity. Cell Mol Life Sci 2012;69:89–102. [PubMed: 21833581]
13. Liu NK, Xu XM. MicroRNA in central nervous system trauma and degenerative disorders. Physiol Genomics 2011;43:571–80. [PubMed: 21385946]
14. Tang W, Cai P, Huo W, Li H, Tang J, Zhu D, Xie H, Chen P, Hang B, Wang S, Xia Y. Suppressive action of miRNAs to ARP2/3 complex reduces cell migration and proliferation via RAC isoforms in Hirschsprung disease. J Cell Mol Med 2016;20:1266–75. [PubMed: 26991540]
15. Chen G, Du C, Shen Z, Peng L, Xie H, Zang R, Li H, Xia Y, Tang W. MicroRNA-939 inhibits cell proliferation via targeting LRSAM1 in Hirschsprung's disease. Aging 2017;9:2471–9. [PubMed: 29253842]
16. Chowdhari S, Sardana K, Saini N. miR-4516, a microRNA downregulated in psoriasis inhibits keratinocyte motility by targeting fibronectin/integrin alpha9 signaling. Biochim Biophys Acta Mol Basis Dis 2017;1863:3142–52. [PubMed: 28844950]
17. Chowdhari S, Saini N. Gene expression profiling reveals the role of RIG1 like receptor signaling in p53 dependent apoptosis induced by PUVA in keratinocytes. Cell Signal 2016;28:25–33. [PubMed: 26518362]
18. Wang Y, Yan W, Wang J, Zhou Y, Chen J, Gu B, Cai W. Common genetic variants in GAL, GAP43 and NRSN1 and interaction networks confer susceptibility to Hirschsprung disease. J Cell Mol Med 2018;22:3377–87. [PubMed: 29654647]
19. Wang Y, Veremeyko T, Wong AH, El Fatimy R, Wei Z, Cai W, Krichevsky AM. Downregulation of miR-132/212 impairs S-nitrosylation balance and induces tau phosphorylation in Alzheimer's disease. Neurobiol Aging 2017;51:156–66. [PubMed: 28089352]
20. Liang CC, Park AY, Guan JL. In vitro scratch assay: a convenient and inexpensive method for analysis of cell migration in vitro. Nat Protoc 2007;2:329–33. [PubMed: 17406593]
21. Ramachandran S, Coffin SL, Tang TY, Jobaliya CD, Spengler RM, Davidson BL. Cis-acting single nucleotide polymorphisms alter MicroRNA-mediated regulation of human brain-expressed transcripts. Hum Mol Genet 2016;25:4939–50. [PubMed: 28171541]
22. Orr N, Chanock S. Common genetic variation and human disease. Adv Genet 2008;62:1–32. [PubMed: 19010252]
23. Li O, Li Z, Tang Q, Li Y, Yuan S, Shen Y, Zhang Z, Li N, Chu K, Lei G. Long Stress Induced Non-Coding Transcripts 5 (LSINCT5) Promotes Hepatocellular Carcinoma Progression Through Interaction with High-Mobility Group AT-hook 2 and MiR-4516. Med Sci Monit 2018;24:8510–23. [PubMed: 30472720]
24. Asahchop EL, Akinwumi SM, Branton WG, Fujiwara E, Gill MJ, Power C. Plasma microRNA profiling predicts HIV-associated neurocognitive disorder. AIDS 2016;30:2021–31. [PubMed: 27191977]
25. Borrelli N, Denaro M, Ugolini C, Poma AM, Miccoli M, Vitti P, Miccoli P, Basolo F. miRNA expression profiling of 'noninvasive follicular thyroid neoplasms with papillary-like nuclear features' compared with adenomas and infiltrative follicular variants of papillary thyroid carcinomas. Mod Pathol 2017;30:39–51. [PubMed: 27586203]

26. Shimojo M, Kasahara Y, Inoue M, Tsunoda SI, Shudo Y, Kurata T, Obika S. A gapmer antisense oligonucleotide targeting SRRM4 is a novel therapeutic medicine for lung cancer. Sci Rep 2019;9:7618. [PubMed: 31110284]

27. Hu Y, Song J, Liu L, Zhang Y, Wang L, Li Q. microRNA-4516 Contributes to Different Functions of Epithelial Permeability Barrier by Targeting Poliovirus Receptor Related Protein 1 in Enterovirus 71 and Coxsackievirus A16 Infections. Front Cell Infect Microbiol 2018;8:110. [PubMed: 29686973]

28. Heanue TA, Pachnis V. Expression profiling the developing mammalian enteric nervous system identifies marker and candidate Hirschsprung disease genes. Proc Natl Acad Sci U S A 2006;103:6919–24. [PubMed: 16632597]

29. Kimberly WT, Zheng JB, Town T, Flavell RA, Selkoe DJ. Physiological regulation of the beta-amyloid precursor protein signaling domain by c-Jun N-terminal kinase JNK3 during neuronal differentiation. J Neurosci 2005;25:5533–43. [PubMed: 15944381]

30. Neidhart S, Antonsson B, Gillieron C, Vilbois F, Grenningloh G, Arkinstall S. c-Jun N-terminal kinase-3 (JNK3)/stress-activated protein kinase-beta (SAPKbeta) binds and phosphorylates the neuronal microtubule regulator SCG10. FEBS Lett 2001;508:259–64. [PubMed: 11718727]

31. Clark AG. The role of haplotypes in candidate gene studies. Genet Epidemiol 2004;27:321–33. [PubMed: 15368617]

32. Kim J, Bartel DP. Allelic imbalance sequencing reveals that single-nucleotide polymorphisms frequently alter microRNA-directed repression. Nat Biotechnol 2009;27:472–7. [PubMed: 19396161]

33. Obermayr F, Hotta R, Enomoto H, Young HM. Development and developmental disorders of the enteric nervous system. Nat Rev Gastroenterol Hepatol 2013;10:43–57. [PubMed: 23229326]

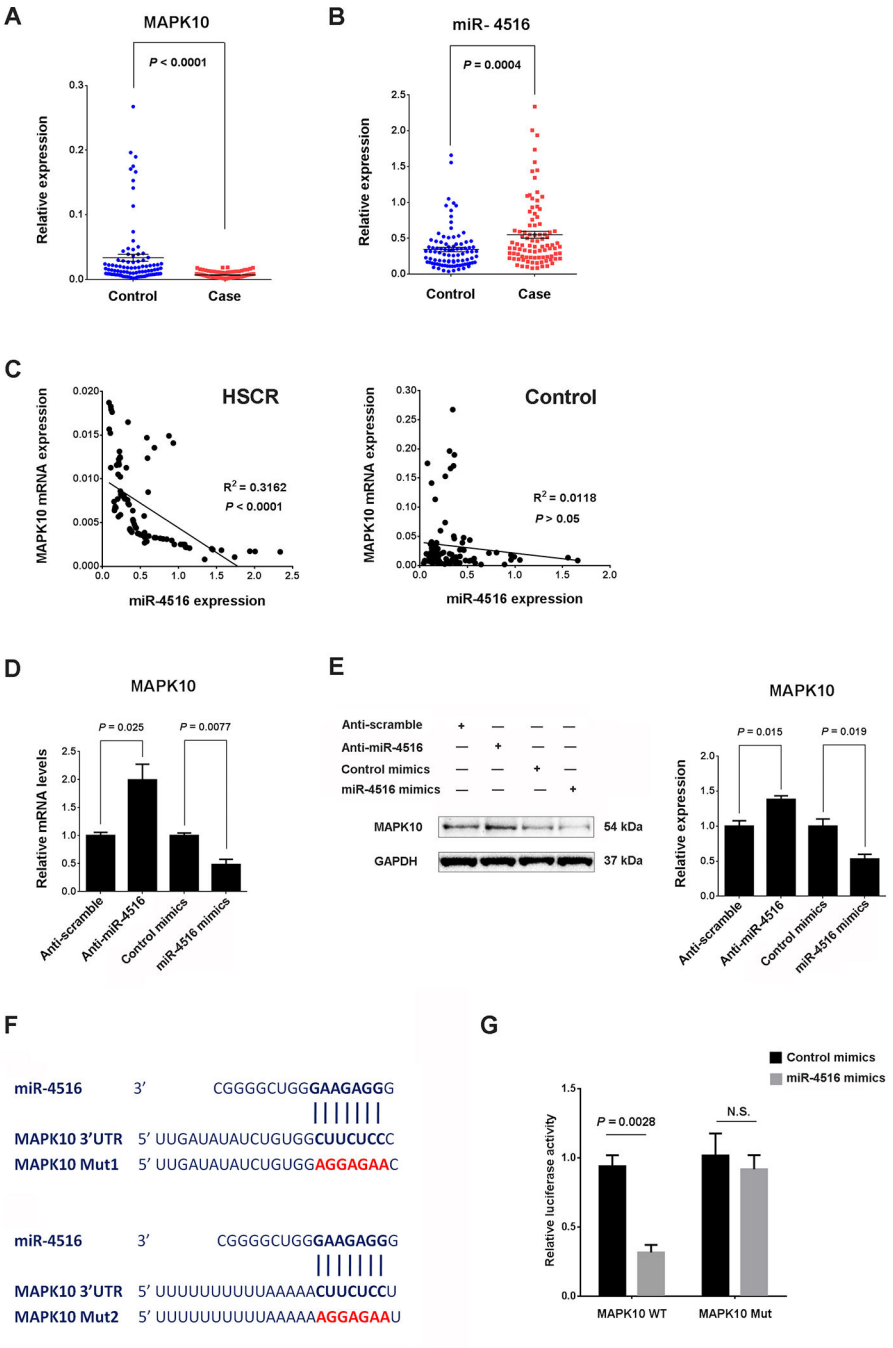

Figure 1.

MAPK10, downregulated in HSCR, is a direct target of miR-4516. (A) (B) The expression levels of *MAPK10* and miR-4516 in 92 HSCR cases and 92 normal controls were assessed by qRT-PCR, and normalized to the uniformly expressed *ACTB* and U6, respectively. (C) The correlation between the levels of MAPK10 and miR-4516. The expression levels were quantified as indicated in (A) and (B). The plots show that miR-4516 inversely correlates with MAPK10 in HSCR tissues (left panel), but not in controls (right panel). (D) (E) The effects of miR-4516 on the expression levels of MAPK10 mRNA and protein in human SH-

SY5Y cells. The levels of mRNA and protein were evaluated by qRT-PCR and Western blotting 72 hours after transfection with either control mimics, miR-4516 mimics, anti-scramble, or anti-miR-4516. Relative mRNA and protein levels were normalized to ACTB and GAPDH respectively. Representative blots are present. (F) The predicted miR-4516 binding sites within the 3'UTR of MAPK10. The mutated sequences in the miR-4516 binding sites are highlighted in red. (G) Relative luciferase activities of the wild-type (MAPK10 WT) or double mutant (MAPK10 Mut) pGL3 promoter vectors co-transfected with either miR-4516 mimics or control mimics into SH-SY5Y cells. (D) (E) (G): Error bar = standard error of the mean, N.S. = not significant, and n = 3. WT, wild type; Mut, mutant.

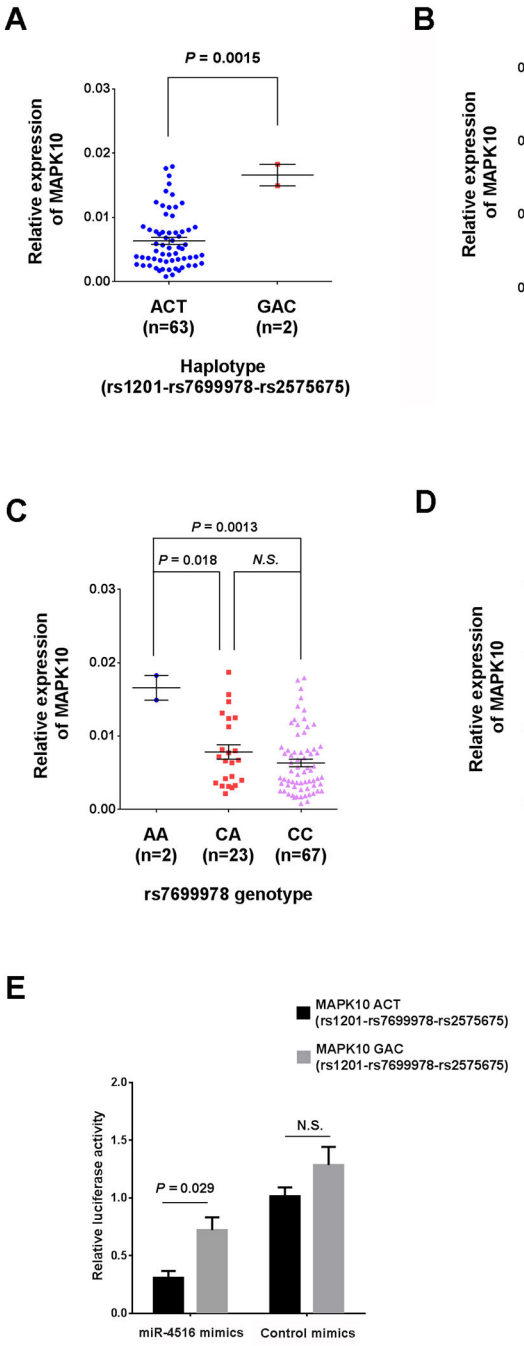

Figure 2.

Cis-acting variants affect miR-4516-mediated regulation of MAPK10. (A) The expression levels of *MAPK10* were interrogated in the HSCR cases carrying the A-C-T or G-A-C haplotype (rs1201-rs7699978-rs2575675). For individual 3'UTR SNPs (rs1201, rs7699978 and rs25755675), the levels of *MAPK10* were further assessed based on the HSCR subjects carrying different genotypes (B) (C) (D). (E) A fragment of human *MAPK10* 3' UTR bearing the A-C-T or G-A-C haplotype (rs1201-rs7699978-rs2575675) was cloned to a pGL3 promoter vector, and co-transfected with either miR-4516 mimics or control mimics

into SH-SY5Y cells. Relative luciferase activities were then evaluated. SNP, single nucleotide polymorphism. Error bar = standard error of the mean, N.S. = not significant, and n = 3.

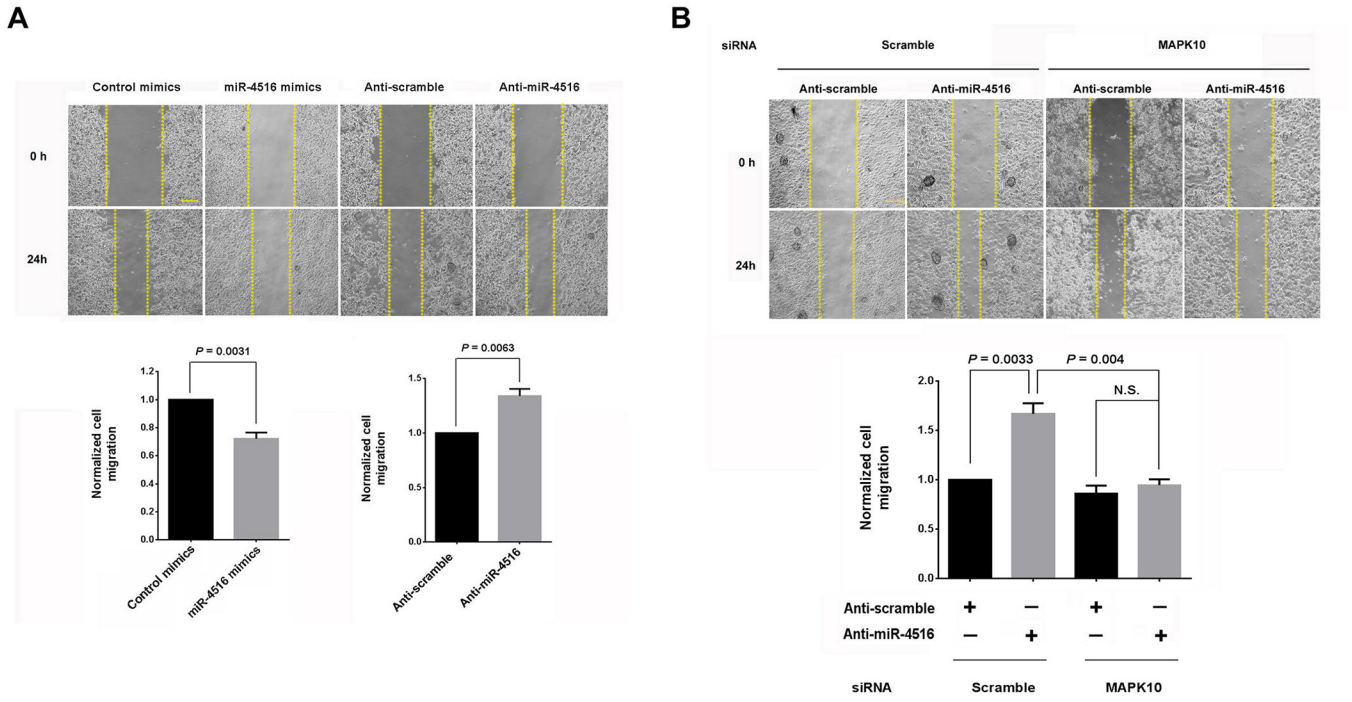

Figure 3.

MiR-4516 modulates the migration of human neural cells in a *MAPK10*-dependent way. (A) Representative images following wound healing assay of SH-SY5Y cells for 24h. Three days after transfection with either miR-4516 mimics, control mimics, anti-scramble, or anti-miR-4516, the confluent transfected SH-SY5Y cells were linear scratch wounded. Incubation was continued for an additional 24h, and images were taken at 0h and 24h. Scale bar = 300 μm. The bottom panel shows quantification of cell migration of SH-SY5Y cells normalized to control mimics or anti-scramble treated cells. (B) Knock-down of MAPK10 rescues the anti-miR-4516 induced increase in cell migration. SH-SY5Y cells were co-transfected with anti-scramble or anti-miR-4516, and control siRNA or siRNA cognate to MAPK10 for 72h. The wound healing assay was performed as described in (A). Representative images are shown, and the bottom panel presents quantification of neural cell migration normalized to anti-scramble treated cells. Error bar = SEM, N.S. = not significant, n = 3.

Table 1.

Allele and genotype distributions of *MAPK10* among HSCR patients and normal controls

SNP ID	Genotype frequency(%)			H-W check *p* value*	*P* value*	FDR adjusted	Allele frequency(%)		X^2	*P* value*	FDR adjusted	Odds Ratio (95%CI)
rs2869444	CC	CG	GG				C	G				
Case	26(5.2)	195(39.0)	279(55.8)	0.279	0.656	> 0.05	247(24.7)	753(75.3)	0.000	0.983	> 0.05	1.00(0.82–1.23)
Control	32(6.2)	189(36.8)	292(56.9)	0.848			253(24.7)	773(75.3)				
rs6823664	CC	CT	TT				C	T				
Case	143(28.9)	234(47.3)	118(23.8)	0.246	0.204	> 0.05	520(52.5)	470(47.5)	1.183	0.277	> 0.05	1.10(0.93–1.31)
Control	123(24.2)	264(51.9)	122(24.0)	0.400			510(50.1)	508(49.9)				
rs12644920	AA	AC	CC				A	C				
Case	30(6.0)	198(39.6)	272(54.4)	0.443	0.719	> 0.05	258(25.8)	742(74.2)	0.134	0.714	> 0.05	0.96(0.79–1.18)
Control	37(7.2)	197(38.6)	277(54.2)	0.808			271(26.5)	751(73.5)				
rs4693765	CC	CT	TT				C	T				
Case	320(64.4)	153(30.8)	24(4.8)	0.307	0.086	> 0.05	793(79.8)	201(20.2)	1.981	0.159	> 0.05	1.17(0.94–1.44)
Control	299(58.5)	191(37.4)	21(4.1)	0.162			789(77.2)	233(22.8)				
rs17449147	AA	AG	GG				A	G				
Case	323(64.5)	155(30.9)	23(4.6)	0.429	0.372	> 0.05	801(79.9)	201(20.1)	2.014	0.156	> 0.05	1.17(0.94–1.44)
Control	310(60.8)	169(33.1)	31(6.1)	0.221			789(77.4)	231(22.6)				
rs10021706	AA	AG	GG				A	G				
Case	363(72.5)	122(24.4)	16(3.2)	0.152	**0.026**	0.170	848(84.6)	154(15.4)	7.625	**0.006**	**0.038**	1.38(1.10–1.74)
Control	331(64.8)	155(30.3)	25(4.9)	0.221			817(79.9)	205(20.1)				
rs1898248	CC	CT	TT				C	T				
Case	302(60.8)	171(34.4)	24(4.8)	0.974	0.094	> 0.05	775(78.0)	219(22.0)	4.613	**0.032**	0.083	1.25(1.02–1.54)
Control	278(54.2)	202(39.4)	33(6.4)	0.647			758(73.9)	268(26.1)				
rs1946733	CC	CT	TT				C	T				
Case	301(60.3)	174(34.9)	24(4.8)	0.858	0.115	> 0.05	776(77.8)	222(22.2)	4.248	**0.039**	0.064	1.24(1.01–1.52)
Control	276(54.1)	201(39.4)	33(6.5)	0.656			753(73.8)	267(26.2)				
rs958	CC	CT	TT				C	T				
Case	294(58.7)	183(36.5)	24(4.8)	0.508	0.089	> 0.05	771(76.9)	231(23.1)	4.624	**0.032**	0.103	1.25(1.02–1.53)
Control	270(52.8)	204(39.9)	37(7.2)	0.856			744(72.8)	278(27.2)				
rs2589515	CC	CG	GG				C	G				

SNP ID	Genotype frequency(%)			H-W check *p* value*	*P* value*	FDR adjusted	Allele frequency(%)		X^2	*P* value*	FDR adjusted	Odds Ratio (95%CI)
Case	24(4.8)	184(36.9)	291(58.3)	0.457	0.097	> 0.05	232(23.2)	766(76.8)	4.292	**0.038**	0.071	0.81(0.66–0.99)
Control	38(7.5)	202(39.6)	270(52.9)	0.979			278(27.3)	742(72.7)				
rs1201	AA	AG	GG				A	G				
Case	302(60.6)	172(34.5)	24(4.8)	0.938	**0.005**	0.067	776(77.9)	220(22.1)	10.558	**0.001**	**0.015**	1.40(1.14–1.71)
Control	262(51.3)	208(40.7)	41(8.0)	0.975			732(71.6)	290(28.4)				
rs7699978	AA	AC	CC				A	C				
Case	15(3.0)	142(28.5)	342(68.5)	0.955	0.108	> 0.05	172(17.2)	826(82.8)	4.393	**0.036**	0.078	0.79(0.63–0.98)
Control	25(4.9)	164(32.0)	323(63.1)	0.481			214(20.9)	810(79.1)				
rs2575675	CC	CT	TT				C	T				
Case	17(3.4)	138(27.7)	343(68.9)	0.500	**0.032**	0.141	172(17.3)	824(82.7)	6.796	**0.009**	**0.040**	0.75(0.60–0.93)
Control	25(4.9)	174(34.0)	313(61.1)	0.897			224(21.9)	800(78.1)				

*Pearson's *p* value, FDR = false discovery rate, SNP = single nucleotide polymorphism, CI = confidence interval, HSCR = Hirschsprung disease.

J Med Genet. Author manuscript; available in PMC 2021 February 11.

Table 2.

Estimated haplotype frequencies and association significance among the 13 SNPs in *MAPK10*

Haplotype*													Haplotype frequency(%)		X^2	*p* value	Odds Ratio (95%CI)
rs2869444	rs6823664	rs12644920	rs4693765	rs17449147	rs10021706	rs1898248	rs1946733	rs958	rs2589515	rs1201	rs7699978	rs2575675	HSCR	Control			
						C		C	G	A	C	T	746.97(76.7)	705.32(69.7)	7.230	**0.007**	1.34(1.08–1.66)
						C				A	C	T	752.95(77.0)	710.15(69.6)	7.925	**0.005**	1.36(1.10–1.68)
								C	G	A	C	T	757.00(76.9)	708.43(70.0)	7.361	**0.007**	1.34(1.08–1.64)
								C		A	C	T	763.00(77.2)	713.36(70.1)	7.842	**0.005**	1.35(1.09–1.66)
									G	A	C	T	757.00(76.9)	708.34(69.9)	7.353	**0.007**	1.33(1.08–1.64)
										A	C	T	764.72(77.4)	714.86(70.1)	13.122	**2.94×10^{-4}**	1.46(1.19–1.79)
G	T	C	C				T	T	C	G	A	C	27.11(2.8)	47.24(4.7)	5.945	**0.015**	0.55(0.34–0.90)
G	C	C	C							A	C	T	263.55(27.2)	226.79(22.5)	4.521	**0.033**	1.25(1.02–1.54)
G	T	C	C	G						G	A	C	24.16(2.5)	42.40(4.2)	5.385	**0.020**	0.55(0.33–0.92)
C	T	A	C	A	G	T	T	T	C	G	A	C	34.38(3.6)	52.23(5.2)	5.005	**0.025**	0.61(0.39–0.94)

*Haplotypes were omitted from analysis if the estimated haplotype probabilities were less than 3%, CI = confidence interval, HSCR = Hirschsprung disease.